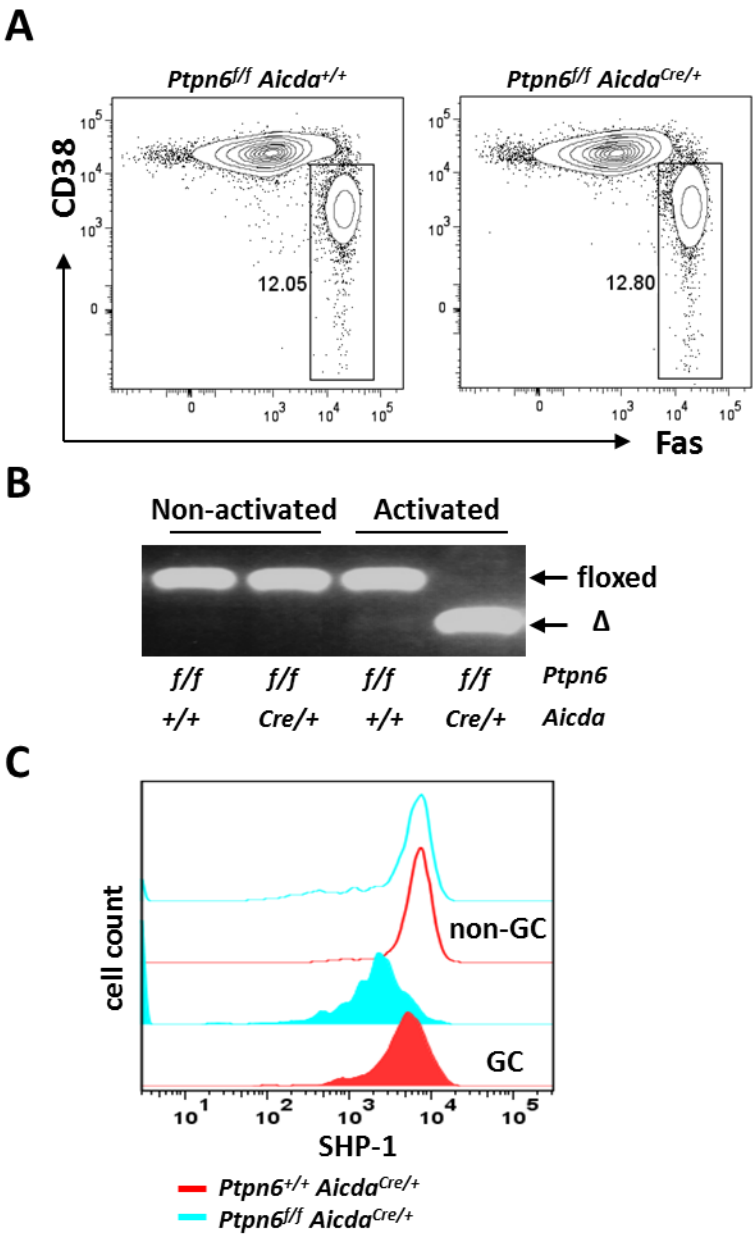

Supplementary Figure 1. AID-Cre-mediated deletion of *floxed Ptpn6* alleles in activated B cells. (A) Flow cytometry analyses of the Peyer's patches (PP) of *Ptpn6*$^{f/f}$*Aicda*$^{+/+}$ and *Ptpn6*$^{f/f}$*Aicda*$^{Cre/+}$ mice depicting germinal center (GC, CD19$^+$Fas$^+$CD38$^-$) and non-germinal center (CD19$^+$Fas$^-$CD38$^+$) B cell populations. Numbers indicate percent of CD19$^+$ cells. (B) Analyses of AID-Cre-mediated deletion of *loxP*-flanked (*floxed*) *Ptpn6* alleles in FACS-sorted activated (CD19$^+$Fas$^+$CD38$^-$) and non-activated (CD19$^+$Fas$^-$CD38$^+$) B cell populations from the PP of *Ptpn6*$^{f/f}$*Aicda*$^{+/+}$ and *Ptpn6*$^{f/f}$*Aicda*$^{Cre/+}$ mice. Genomic DNA was subjected to PCR analysis using primers as documented previously[17]. Bands corresponding to the floxed and deleted (D) *Ptpn6* alleles are indicated. (C) Flow cytometry analyses of intracellular Shp1 protein expression in activated (shaded histogram) and non-activated (unshaded histogram) cells from PP of *Ptpn6*$^{+/+}$*Aicda*$^{Cre/+}$ (red histogram) and *Ptpn6*$^{f/f}$*Aicda*$^{Cre/+}$ (blue histogram) mice. Data are representative of three independent experiments.

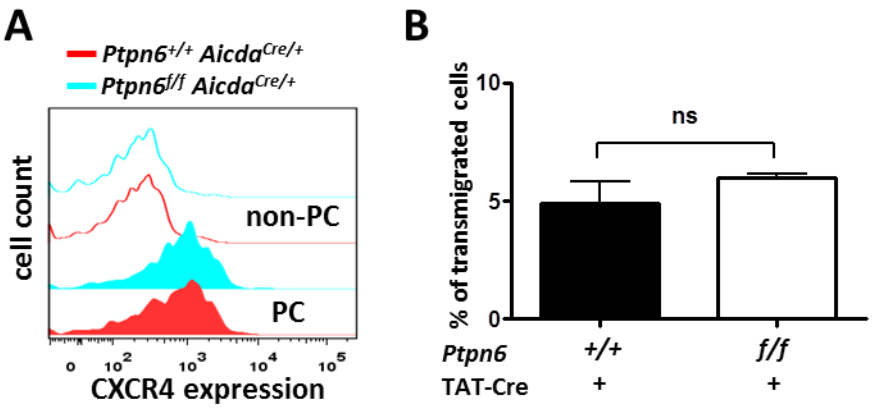

Supplementary Figure 2. CXCR4 expression and responsiveness of Shp1-deficient PC.
Plasma cells from mice challenged with NP_{38}-CGG were analyzed at day 10 post-immunization for the expression and function of CXCR4. (A) Flow cytometry analyses of CXCR4 expression on PC (shaded histogram) and non-PC (unshaded histogram) from immunized *Ptpn6*$^{+/+}$*Aicda*$^{Cre/+}$ (red histogram) and *Ptpn6*$^{f/f}$*Aicda*$^{Cre/+}$ (blue histogram) mice. Histograms were overlaid for direct comparison. (B) Transmigration of FACS-sorted *Ptpn6*$^{+/+}$ and *Ptpn6*$^{f/f}$ plasma cells examined in transwell assay with lower chamber containing 2 µg/mL SDF-1a, ns=non-significant. Data are representative of three independent experiments.

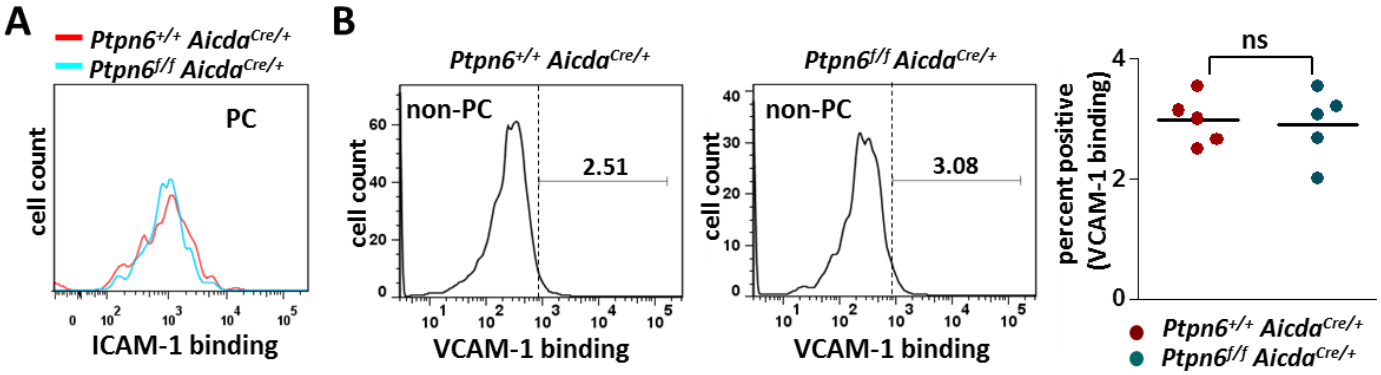

Supplementary Figure 3. Examination of ICAM-1 and VCAM-1 binding.
(A) Flow cytometry analysis of soluble ICAM-1-Fc (20 µg/ml) binding by PC from immunized *Ptpn6*$^{+/+}$*Aicda*$^{Cre/+}$ (red histogram) and *Ptpn6*$^{f/f}$*Aicda*$^{Cre/+}$ (blue histogram) mice. (B) Flow cytometry analysis of soluble VCAM-1-Fc (20 µg/ml) binding by non-PC from immunized *Ptpn6*$^{+/+}$*Aicda*$^{Cre/+}$ (left panel) and *Ptpn6*$^{f/f}$*Aicda*$^{Cre/+}$ (middle panel) mice and quantification of the percentage of cells that bind VCAM-1 (right panel). Each circle represents data obtained from one mouse examined; ns=non-significant.

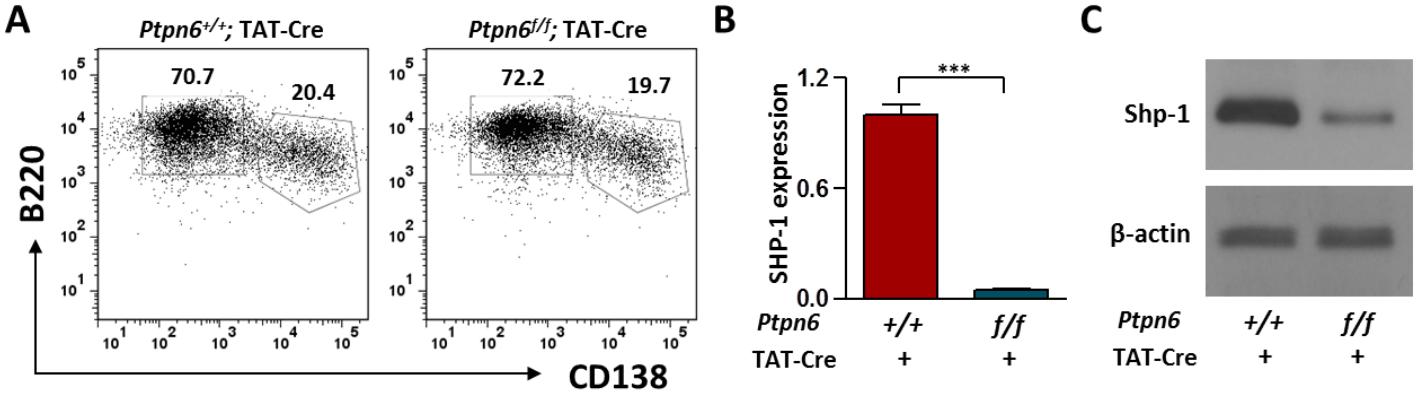

Supplementary Figure 4. Examination of plasma cell differentiation and efficiency of Shp1 deletion. (A) Flow cytometry analysis of LPS-induced differentiation of plasma cells from purified splenic B cells obtained from *Ptpn6*$^{+/+}$ and *Ptpn6*$^{f/f}$ mice and transduced with Tat-Cre. (B) Quantitative qRT-PCR analysis of Shp1 mRNA and (C) western blot analysis of Shp1 protein, expression in FACS-sorted plasma cells. *b-actin* served as normalization and loading control in B and C. Data are representative of at least three independent experiments.

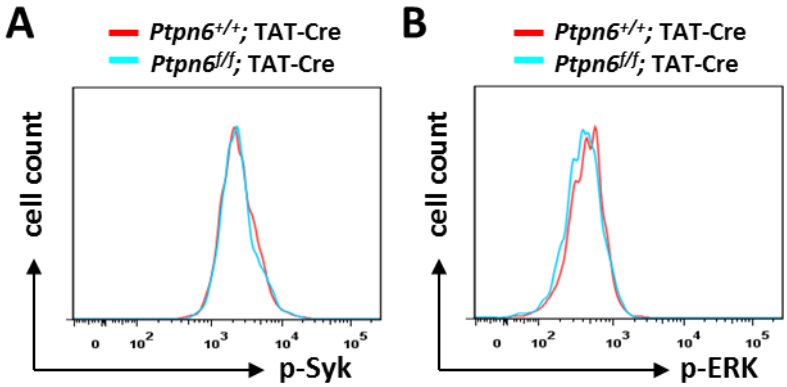

Supplementary Figure 5. Examination of phospho-Syk and phospho-ERK content in Shp1-deficient plasma cells.

Intracellular flow cytometry stainings of (A) phospho-Syk and (B) phospho-ERK content in Tat-Cre-transduced LPS-differentiated plasma cells from *Ptpn6*$^{+/+}$ (red histogram) and *Ptpn6*$^{f/f}$ (blue histogram) mice. Data are representative of at least three independent experiments.

Expanded blot for Figure 7a

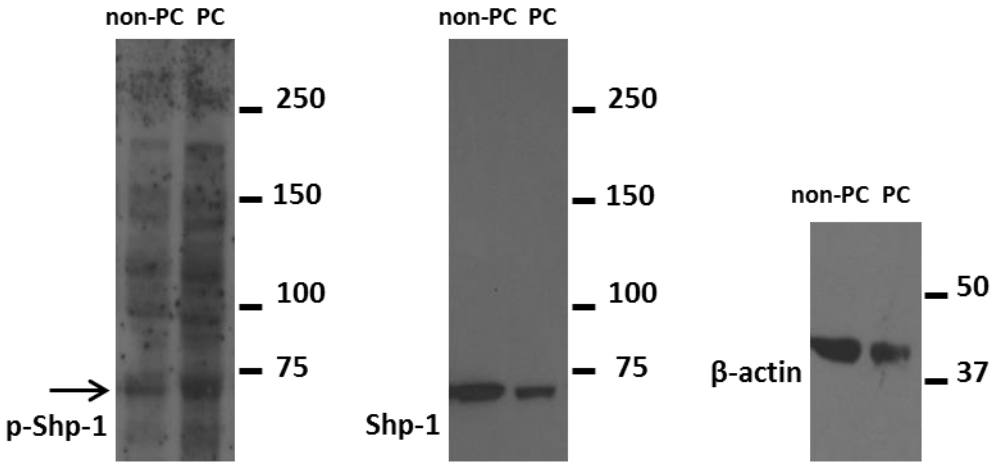

Expanded blot for Figure 9a

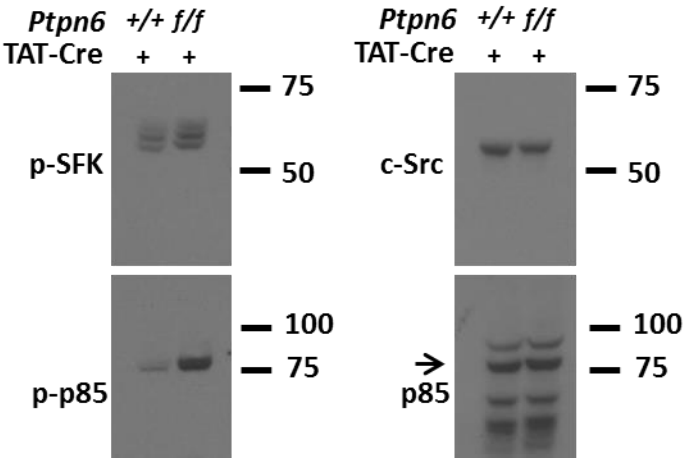

Supplementary Figure 6. Extended Western blots for results shown in Figures 7a and 9a.